



This project is part of the PRIMA  
programme supported by the  
European Union

## **PRIMA-SECTION 2-2022**

### **“Modelling and Technological Tools to Prevent Surface and Ground-Water Bodies from Agricultural Non-Point Source Pollution Under Mediterranean Conditions”**

**NPP-SOL**

**Report on designing Drainage System and BR**

**Deliverable number: D.2.1**

# Non-Point Pollution SOLutions (NPP-SOL)

Deliverable number: D.2.1

## Report on designing Drainage System and BR

---

Author(s)	A. Coppola (University of Basilicata – University of Cagliari) A. Comegna (University of Basilicata) S. B. M. Hassan (University of Basilicata)
-----------	---

---

Approved by reviewers

---

Date of approval

---

Approved by project coordinator

---

Date of approval

---

Call	PRIMA Section 2 2022- Multi-topic Topic 2.1.1 RIA (Prevent and reduce land and water salinization and pollution due to agri- food activities).
------	---

---

Project URL: <https://npp-sol.iamm.ciheam.org/>

---

## 1. Introduction

Bioreactors (BR) for agricultural source pollutants are *in situ* bioremediation passive treatment systems that can be used to remove nitrates, phosphorus (and even pesticides) from both surface runoff water and shallow groundwater by intercepting the percolation and/or runoff flows of water and dissolved pollutants through a drainage system. A BR is commonly constructed as a large, lined trench (or container) filled with a carbon-rich porous material (generally with woodchip), which is designed to collect runoff water or tile drainage for treatment (Christianson and Schipper, 2016; Moorman et al., 2010).

With these systems, the reduction of nutrients and pesticides may be obtained by making part of the drainage and/or runoff volumes flow through an artificial porous medium containing woodchip (high C:N ratio for heterotrophic denitrification process), mixed with activated alumina/gravel mixture (for phosphate precipitation and complexation). Biochar-amended BRs are also able to remove pesticides. These treatment systems are characterized by relatively low construction costs, ensuring relatively high levels of nitrate removal from the treated water. In a study comparing seven methods for cleaning water contaminated with nitrates, Christianson et al. (2013) concluded that bioreactor-based methods were cost-effective and highly efficient. Likewise, a more recent report by various Iowa state agencies, which examined different edge-of-field practices (including wetlands, buffers, bioreactors, and controlled drainage), found that woodchip bioreactors were the most economical option for reducing nitrogen, based on the cost per unit of nitrogen removed (IDALS, IDNR, ISUCALS, 2017).

This is why BR is nowadays one of the most promising and widespread bioremediation technologies for groundwater and surface water networks.

Bioreactors can be built at the edges of cultivated fields or along access roads to fields. They can also be covered with soil on the surface, thus not interfering with agricultural work and operations. They can also be built directly in a buffer strip or watercourse when the water to be treated predominantly comes from surface runoff. They are particularly interesting because they can be implemented in a decentralized manner (at the farm scale), allowing individual fields to intercept pollutants flows moving toward the groundwater or surface water network, thus reducing the spread of groundwater and surface water pollution. Additionally, since they need to be equipped with proper monitoring systems at both the inlet and outlet, these bioreactors allow individual farmers to assess the effectiveness of their irrigation and fertilization practices based on the nutrient loads entering the bioreactor over time and to make necessary adjustments in water and nutrient management.

Before presenting the design criteria and parameters, this section will cover the fundamentals of pollutant removal mechanisms and mathematical modeling in BR. This background is crucial for understanding the reasoning behind the design criteria and parameters and the method to evaluate the hydraulic performance of the designed BRs, which will be discussed in the second part of this report.

## 2. Pollutant removal mechanism

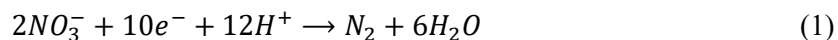
### 2.1. Nitrate removal mechanism

Traditionally, BRs have been primarily implemented in agricultural environments to address the remediation of nitrates from tile drainage and runoff water (Christianson et al., 2017; Sarris and Burberry, 2018). The removal of nitrate is principally driven by denitrification, a microbial process that gradually reduces nitrate to nitrite, nitric oxide, nitrous oxide, and ultimately dinitrogen ( $N_2$ ) gas. BRs are specifically thought to stimulate and amplify natural biological nitrate degradation processes by providing a carbon substrate for denitrifying microorganisms. Woodchip, or any other cheap carbon material, serves as a surface for complex microbial biofilm formation in bioreactors, offering a readily available, sustainable, and cost-effective carbon source (coming from the hydrolysis of the polymeric organic carbon substrate) that can last for several years (Christianson et al., 2010; Coleman et al., 2019; Robertson and Merkley, 2009). Carbon substrates with a high C:N ratio are required.

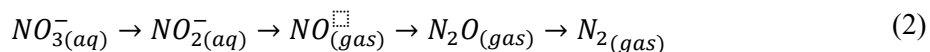
In unsaturated conditions, facultative anaerobes bacteria (microorganisms that can carry out metabolic activity under the presence and absence of oxygen, e.g., both aerobic and anaerobic conditions) use oxygen to oxidize available carbon. As oxygen levels become scarce, facultative anaerobes shift to using N oxides ( $NO_x$ ,  $N_2O$ ) as electron acceptors in their respiration electron transport chain. The biomass, consisting of colonies of heterotrophic bacteria naturally present in the soil and the cortical part of the filling material, under the appropriate process conditions ( $ORP \leq -50$  to  $+50$  mV;  $pH = 5.5-8$ ;  $T = 25-35^\circ C$ ;  $DO \leq 2$  mg/l), uses nitrates to oxidize the carbonaceous substrate, which serves both as an energy source for the metabolic activities of the biomass (denitrifying bacteria use denitrification to generate ATP) and as an electron donor.

The following reaction chain, in which specific catalytic enzymes are involved under anaerobic conditions, sequentially reduces nitrates to nitrogen gas:

The overall half-reaction of the process of denitrification reaction is:

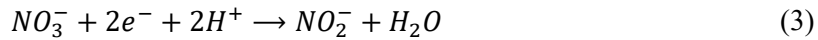


This reaction involves a four-step chain.

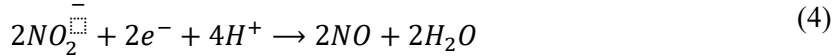


with each step being catalyzed by specific enzymes:

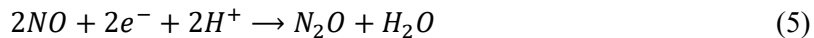
1. Conversion of nitrate to nitrite, catalyzed by *nitrate reductase (Nar)*:



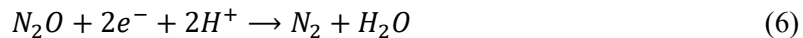
2. Conversion of nitrite to nitric oxide, catalyzed by *nitrite reductase* (*Nir*):



3. Conversion of nitric oxide into nitrous oxide, catalyzed by *nitric oxide reductase* (*Nor*):



4. Conversion of nitrous oxide into dinitrogen, catalyzed by *nitrous oxide reductase* (*Nos*):



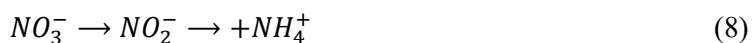
Denitrifying bacteria use denitrification to generate ATP. During denitrification, the microbial community utilizes nitrate or denitrification intermediates (NOx) as terminal electron acceptors for respiration, coupling the reductive process to the oxidation of a carbon-based electron donor under anaerobic conditions (Greenan et al., 2006; Rich et al., 2003; Schipper et al., 2010):



The end products of denitrification include N<sub>2</sub>, carbon dioxide (CO<sub>2</sub>), and bicarbonate (HCO<sub>3</sub><sup>-</sup>) (eq. 7): The predominant nitrogenous end product, N<sub>2</sub>, is stable due to its molecular triple bonds. The HCO<sub>3</sub><sup>-</sup> can be important because this alkalinity release increases the solution pH (Metcalf and Eddy, 2003).

Once nitrates are nearly completely reduced, obligate anaerobes become active and begin using other electron acceptors, such as sulfate (SO<sub>4</sub><sup>2-</sup>), manganese (Mn (IV)), and iron (Fe (III)). The sequence of these reactions depends on the amount of free energy released, with denitrification, for instance, releasing more energy than sulfate reduction (Metcalf and Eddy, 2003).

Besides denitrification, other microbial processes have been observed in BR systems, such as *dissimilatory nitrate reduction to ammonia* (DNRA) and *anaerobic ammonium oxidation* (*anammox*). DNRA may produce ammonia nitrogen in woodchip bioreactors (Martin et al., 2019). In this process, microbes involved in DNRA oxidize organic matter and use nitrate (instead of oxygen) as an electron acceptor, reducing it first to nitrite, and then to ammonium, following this reaction chain:



even if the reaction may start with NO<sub>2</sub><sup>-</sup> directly.

*Anammox* is a microbial process that can produce N gases ( $N_2O$  and  $N_2$ ) by oxidizing ammonium  $NH_4^+$  with  $NO_3^-$  or nitrite ( $NO_2^-$ ) under strictly anoxic conditions (Griesmeier et al., 2017). *Anammox* process is catalyzed by members of the Planctomycetales. Here, ammonium serves as an electron donor, and nitrite as an electron acceptor. Dinitrogen is formed as the end-product according to the following reaction:



This process may result in effective nitrogen removal, particularly in field denitrification beds designed to treat water with high ammonium levels.

However, previous researches based on microbial community analysis have shown limited potential for anammox, even if high concentrations of both  $NO_3^-$ -N and  $NH_4^+$ -N can activate both denitrification and anammox processes (Rambags et al., 2019).

## 2.2. Phosphorus removal mechanism

The effectiveness of woodchip bioreactors (BRs) in removing phosphate ( $PO_4^{3-}$ ) from agricultural runoff has been studied, but the results regarding their efficiency are somewhat unclear (Soupis et al., 2018). Generally, denitrifying woodchip bioreactors have shown promise in removing phosphorus. Sanchez Bustamante-Bailon et al. (2024) analyzed the levels of dissolved reactive phosphorus (DRP) entering and leaving ten bioreactors in Illinois and found that this form of phosphorus was often removed by the BRs (Sanchez Bustamante-Bailon et al., 2024).

However, phosphorus release from the woodchip has been observed when the BR is new or during low-flow conditions, which could result in a potential pollution tradeoff. Even if this release is diluted by mixing with receiving water, the resulting concentration might still exceed water quality guidelines for preventing eutrophication in freshwater ecosystems. This release is linked to the phosphorus content initially present in the woodchip, which can range from 0.013% to 0.20% (Christianson et al., 2022). Some of this phosphorus can become solubilized, particularly during the initial saturation of the media at startup, when dissolved phosphorus concentrations in bioreactor outflows have been observed to even exceed 1.0 mg P/L (von Ahnen et al., 2016; Sanchez Bustamante-Bailon et al., 2024; Rivas et al., 2020;). Despite the risk of phosphorus leaching, BR phosphorus removal after the startup period has been increasingly documented. Gottschall et al. (2016) and White et al. (2022) both reported dissolved phosphorus removal by bioreactors, averaging 35%–45%. Moderate but still positive removal efficiencies ranging from 5% to 17% have been observed in lab-scale woodchip studies (Hua et al., 2016).

The mechanisms for phosphorus removal in bioreactors include: 1) physical filtration, 2) chemical adsorption, and 3) microbial immobilization (Hua et al., 2016). 1) Woodchip bioreactors serve as a physical filter for particulate phosphorus, though the precise mechanisms for dissolved phosphorus removal are less well understood. 2) Sorption of dissolved phosphorus by the woodchips may also play

a role. The potential involvement of metal elements in the wood, such as calcium (Ca), magnesium (Mg), aluminum (Al), and iron (Fe), in capturing phosphorus through precipitation or ligand exchange has also been investigated (Sanchez Bustamante-Bailon et al., 2022). These four metals would each be present in bioreactor woodchip media, though in varying concentrations depending on tree species and environmental growth conditions

Since phosphorus removal from water occurs through sorption or precipitation reactions, specific studies have carried out with woodchip bioreactors that also includes phosphorus-sorptive media, such as biochar, industrial residuals containing aluminum (Al), steel turnings, or steel byproducts (Zoski et al. 2013; Goodwin et al. 2015; Hua et al. 2016; Coleman et al., 2019). For example, Gottschall et al. (2016) found that woodchips amended with aluminum/iron/calcium-based sludge from water treatment plants increased the total phosphorus removal to over 50%, from the 30% obtained by a simple woodchip bioreactor.

Husk et al. (2018) studied the effectiveness of bioreactors containing either woodchips alone or a combination of woodchips and an activated alumina/gravel mixture (mixed media). The study concluded that the bioreactor with the activated alumina/gravel mixture has a higher phosphorus sorption capacity and should be considered as part of an integrated system for simultaneous nitrogen and phosphorus removal from agricultural drainage.

### 2.3. Pesticides removal mechanism

In the last decade, research has also been carried out to investigate the capability of woodchip BR to attenuate other pollutants possibly present in agricultural drainage, such as pesticides (Ilhan et al., 2011). In general, removing pesticides from agricultural runoff may be achieved by sequestering the pesticides using filters with a carbon source, followed by some microbial degradation. In this regard, woodchip bioreactors (BRs) may act as a sorbent material for specific pesticides, while also promoting a bacterial community that aids in their degradation (Camilo et al., 2013).

Hunter and Shaner (2010) recommended two sequential bioreactors, where the anaerobic bioreactor removes nitrates and a subsequent aerobic one degrades atrazine in aqueous solution.

However, adding biochar to the woodchip BR has been found to significantly increase the pesticide sorption characteristics. Biochar is generally characterized by a relatively low bulk density. Besides, it is characterized by surface features, such as high specific surface area, high surface charge density, and a large micropore volume with both polar and nonpolar surface sites, all making it a strong sorbent and enabling it to adsorb organic molecules and nutrients (Laird et al., 2010).

## 3. Pollutant removal modelling in denitrifying bioreactors

As mentioned earlier, modeling the hydraulic behavior and pollutant removal in a BR is crucial for designing an optimal system that maximizes denitrification while minimizing secondary, potentially harmful reactions. First and foremost, modeling the hydraulic characteristics of a BR is necessary to determine how long a given volume of water will stay within the bioreactor. This retention time, in turn,

is closely related to the degree of treatment achieved, based on the relevant reaction kinetics (Metcalf and Eddy, 2014). Comparing a BR's actual hydraulic characteristics, for example, using tracers, with the expected theoretical response can help assess how closely the system aligns with the ideal design. This comparison allows for the evaluation of the effectiveness of the design in achieving optimal hydraulic performance.

The denitrification bed model comprises two components: water flow and nitrate removal kinetics. Regarding the former, we proved that Forchheimer's equation best describes water flow through woodchips (Ghane et al., 2014) which is written as:

$$-J = \frac{q_w}{K_s} + \beta q_w^2 \quad (10)$$

where  $q_w$  is the specific discharge (cm/sec),  $J$  is the hydraulic gradient (cm/cm),  $K_s = \frac{k_p \gamma}{\mu}$  is the saturated hydraulic conductivity (cm/sec) and  $\beta$  a constant ( $s^2/cm^2$ ). The hydraulic gradient is calculated as the ratio of hydraulic head difference,  $\Delta H$  (cm), between the inflow ( $H_i$ ) and outflow ( $H_o$ ) water heights to the BR bed length,  $L$  (cm).  $K_p$ ,  $\mu$  and  $\gamma$  are respectively the intrinsic permeability ( $cm^2$ ), the water dynamic viscosity ( $g/cm^2/s$ ) and the specific weight of the water ( $g/cm^3/s^2$ ).

The first and second terms on the right-hand side of equation 10 approximately represent the contributions of viscous and inertial forces (flow resistance), respectively. It is evident that when the specific discharge is low enough, the inertial force can be neglected, and the equation simplifies to Darcy's law. Conversely, when the specific discharge is high enough, the viscous force becomes negligible, and the equation represents a fully developed turbulent flow.

Solving the quadratic equation 10, and replacing  $J = \Delta H / L$  results in only one practical solution as Ghane et al.,

$$q_w = \frac{-\frac{1}{K_s} \sqrt{\left(\frac{\mu}{k_p \gamma}\right)^2 - 4\beta \left(\frac{\Delta H}{L}\right)}}{2\beta} \quad (11)$$

The theoretical hydraulic retention time,  $t_t$  (cm/h), is obtained as:

$$t_t = \frac{V_s \phi}{Q} = \frac{L \phi}{q_w} \quad (12)$$

where  $V_s = AL$  is the saturated volume of the bed,  $Q = q_w A$  is the discharge rate,  $\phi$  is the total porosity available for flow through woodchips,  $V_s$  and  $A$  being, respectively, the saturated volume of the BR bed and the mean cross-sectional area.

Combining the two equations above results in the following equation for the theoretical time (in hours):

$$t_t = -\frac{2\beta L\phi}{3600 \left( -\frac{1}{K_s} \sqrt{\left( \frac{\mu}{k_p \gamma} \right)^2 - 4\beta \left( \frac{\Delta H}{L} \right)} \right)} \quad (13)$$

Enzyme catalyzed nitrate removal rate in woodchip bioreactors can be described by a dual-substrate Michaelis-Menten model (Halaburka et al., 2017):

$$R_N = R_{N,max} \frac{C_{in,C}}{K_{M,C} + C_{in,C}} \frac{C_{in,N}}{K_{M,N} + C_{in,N}} \quad (14)$$

where  $R_N$  is the nitrate removal rate (mg N/L/h),  $R_{N,max}$  is the maximum removal rate (mg N/L/h),  $C_{in,C}$  is the initial (or at BR inlet) concentration of dissolved organic carbon (DOC) (mg C/L),  $C_{in,N}$  is the initial concentration of nitrate (mg N/L),  $K_{M,C}$  and  $K_{M,N}$  are the Michaelis-Menten half saturation constant (that is the concentration at which nitrate removal rate is half the maximum rate) (mg C/L or mg N/L), respectively for DOC and nitrate.

By assuming that the release rates of biodegradable organic carbon from woodchips remain relatively stable during each kinetics experiment, the following simplified, single-substrate Michaelis-Menten model can be used to describe nitrate removal rates for each kinetics experiment:

$$R_N = \frac{R_{N,max} C_{in,N}}{K_{M,N} + C_{in,N}} \quad (15)$$

which can also be simply seen as the difference between the BR inflow and outflow nitrate concentrations ( $C_{in,N} - C_{out,N}$ ) divided by the time,  $t_t$ , it takes for the nitrate removal to occur:

$$R_N = -\frac{C_{out,N} - C_{in,N}}{t_t} \quad (16)$$

Finally, the outflow concentration under steady-state flow can thus be obtained by combining equations 13, 15 and 16:

$$C_{out} = -\frac{R_{N,max} C_{in,N}}{K_{M,N} + C_{in,N}} \frac{2\beta L\phi}{3600 \left( -\frac{1}{K_s} \sqrt{\left( \frac{\mu}{k_p \gamma} \right)^2 - 4\beta \left( \frac{\Delta H}{L} \right)} \right)} + C_{in} \quad (17)$$

$R_{N,max}$  and  $K_{M,N}$  may be obtained directly from nitrate removal rates observations at different inlet concentrations,  $C_{in}$ , respectively by the intercept and the slope of the straight line resulting from the inversion of equation 15:

$$\frac{1}{R_N} = \frac{K_{M,N}}{R_{N,max}} \frac{1}{C_{in}} + \frac{1}{R_{N,max}} \quad (18)$$

Note that at high nitrate concentration ( $C_{in} \gg K_{M,N}$ ) the equation 15 approximates a zero order reaction, with  $R_N \approx R_{N,max}$ , whereas at low nitrate concentrations ( $C_{in} \ll K_{M,N}$ ) it approximates a first-order reaction, with  $R_N \approx R_{N,max} C_{in} / K_{M,N}$ .

## 4. Designing a Bioreactor System

### 4.1. Design and construction

The BR system proposed in the project aims at a progressive reduction (in the medium term) of nitrate concentrations in the groundwater through the partial interception of percolation flows of water and dissolved nitrates through a drainage system, partly already existing and made up of open and part to be created with underground tubular drains. The reduction of nitrates is achieved by flowing part of the drained volumes into a bioreactor where a (natural) complete denitrification occurs (from nitrate to molecular nitrogen). Compared to any other type of treatment involving already polluted water (stripping, for example), the interception of the nitrate flows for drainage. The subsequent passage through a bioreactor allows the problem to be solved upstream, when the pollutant has not yet spread to the groundwater, significantly reducing the volumes to be treated.

Within NPP-SOL, BRs have been built using Italian and Israeli case studies. In Israel, a BR physical model treating only surface water has been assembled at an experimental scale, mainly for research exploration (see Figure 1).



Figure 1. The bioreactor in Israel. From top left clockwise: the excavated pit for the bioreactor, lining the bioreactor internal wall, filling the bioreactor with the media and, finally, covering with soil

By contrast, in Italy the BR construction has been carried out to be immediately operative at farm scale in four different sites made available by local farmers, where each BR serves an average area of 15 hectares (see Figure 2).

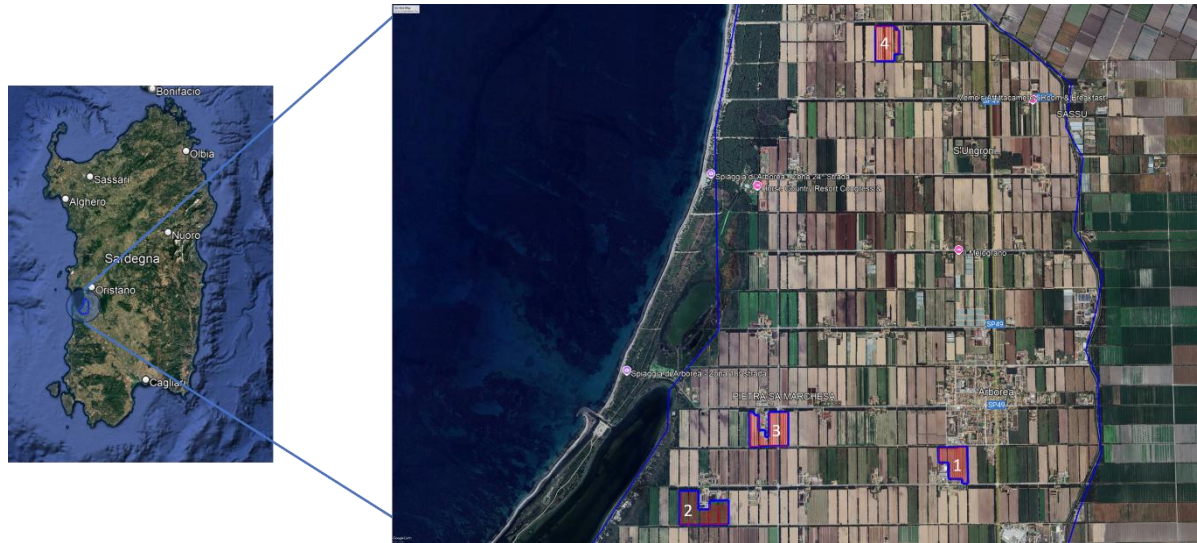


Figure 2. The study area is in Arborea, Sardinia, Italy.

A key challenge in designing agricultural drainage bioreactors is the considerable fluctuation in drainage flow rates throughout the year, which causes variable bioreactor retention times (see equation 12). This variability imposes the design of a BR to balance the need to treat a significant portion of the annual drainage volume by ensuring sufficient retention times at all flow rates for optimal nitrate removal while also considering cost-effectiveness. Designing denitrification bioreactors based on peak drainage flow rates could result in an impractically extensive system, as most sites would need an oversized bioreactor to handle 100% of annual drainage flow, which would be too large for the relatively low flow rates observed during much of the year. This is why a common approach to BR design is sizing the BR to treat a percentage of annual drainage volume. This is, for example, the approach adopted by Christianson et al. (2011), who use a BR design method to obtain a 4-h retention time at a design flow rate of 20% of the estimated peak flow rate.

Estimating the peak flow rate is crucial for designing bioreactors. Several methods exist for estimating peak flow rates that align with the 20% design criterion. The ideal approach would be to gather a series of peak flow observations over multiple years, providing a reliable basis for estimating the design peak flow. However, this method requires an existing drainage system to monitor the flow rates. Alternatively, two commonly used methods are: 1) applying a drainage coefficient (DF) in mm/day, which estimates the theoretical maximum water drainage rate from a field per day and is multiplied by the drainage area to provide the estimated peak flow, and 2) using Manning's (or Chezy's) resistance equation for estimating mean flow velocity in pipes and thus calculating the maximum capacity of the drainage outlet by selecting an appropriate Manning's  $n$  value (for the Manning equation) or Gauckler-Strickler value (in the case of Chezy's equation). These approaches are beneficial when the drainage system has not yet been installed, as seen in the Italian case study, where the drainage system design was developed alongside the BR design.

To generalize, when the drainage system does not exist yet, BRs construction involves the following steps:

1. Installing the drainage network and collectors to address drainage fluxes to BRs;
2. Building the BRs and related hydraulic and electromechanical works;
3. Installation of monitoring equipment.

In the following, each of these items will be described in detail, assuming the drainage system does not exist, as in the Italian case study. This is why the Arborea case study will be used as an example of drainage system design.

#### 4.2. Drainage Network and Collectors

To collect surface groundwater and remove nitrate-rich percolated water, a horizontal drainage network must be installed, with drains consisting of perforated polyethylene.

In designing the drainage system, the following steps should be theoretically followed:

1. Create a topographic map of the fields showing the potential drain outlet's elevations and defining the drains' installation depth. In the Arborea Plain area (the Italian case study), which is a hydraulically reclaimed area, the elementary field is approximately 4 hectares in size (400m x 100m), often bordered by free-surface drains placed along rows of eucalyptus trees. In this case, the topographic map was created by a GPS;
2. Defining the layout of the drainage system. Due to the regular shape of the fields in the area, a parallel design was used in the Arborea plain, with the subsurface drainage pipes lying parallel to the long side of each plot and collectors placed normal to the drains and along the shorter side of the field;
3. Defining the drain spacing and depth. Both these design parameters have to be simultaneously determined according to the target (predetermined) depth of groundwater. Once this depth is fixed, the Hooghoudt (1940) theory for lateral flow and transport to the drains can be applied. This theory links the depth and spacing of parallel subsurface drains with factors such as the water table's depth, the soil layers' thickness, and their saturated hydraulic conductivity. Using this theory, the appropriate depth and spacing for drain installation can be calculated;
4. Defining the drain diameter. This depends on the discharges to be drained by each drain, which in turn depends on the drain spacing, length, slope, and pipe wall roughness, as well as the drainage coefficient, DF;
5. Defining the diameter of the collectors. This depends again on the discharge to be collected (the sum of discharges coming from the lateral drains, along with the same factors as in the previous item);

In the specific case of Israel, the drainage system consists of surface water during the winter and treated wastewater during the summer. In the particular case of Arborea Plain, the design of drainage systems, in terms of installation depth, has been slightly different according to the specific strategy adopted in the NPP-SOL technology strategy, aiming at intercepting the pollutants fluxes, originating from both

organic and mineral fertilizers and coming from the soil surface before their spreading into the groundwater. To do that, the drains were placed from the beginning precisely at the water table depth, allowing the flows of pollutants to be diverted towards the BR as soon as they reach the water table. A preliminary analysis of a three-year series of depth-to-water table was carried out for each site identified for BR installation. This allowed us to verify that the water table oscillations mainly were around 90 cm, with a minimum of 110 cm. Accordingly, the design drain installation depth was fixed at 100 cm, with a spacing of 20 m, based on the application of the Hooghoudt approach and the measured soil-saturated hydraulic conductivity. This type of installation allows the drain to activate immediately as soon as the water (and solute) moving downward reaches the water table, thus minimizing the spreading of the solute into the groundwater. This mechanism is schematized in Figure 3.

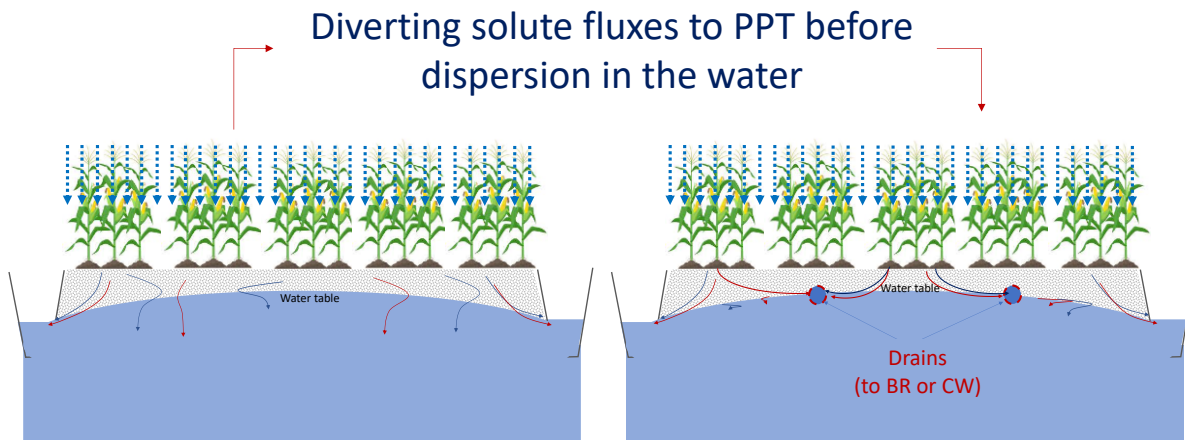


Figure 3. Schematic view of the interception of water and nutrients by artificial drainage before spreading into the groundwater.

Considering a DF of about 12 mm/d and an average size of the field to be drained of 16 ha (4 elementary fields), a theoretical peak drainage volume of 1920 m<sup>3</sup>/d was calculated. By assuming the treatment of about 20% of this theoretical drainage (384 m<sup>3</sup>/d) by the BR, a total flux of 4.45 l/s was obtained and considered for the sizing of the BR. Assuming a drain slope of 1‰, this flux also allowed us to calculate the drain's diameter by inverting Chezy's resistance equation for water flow velocity in pipes.

$$v = \chi \sqrt{RJ} \quad (19)$$

$$\chi = C_s R^{1/6}$$

where  $\chi$  is the Chezy's coefficient (m<sup>1/3</sup>/s), determined by the Gauckler-Strickler relationship involving the Strickler roughness coefficient,  $C_s$ , in our case fixed at 90 m<sup>1/3</sup>·s<sup>-1</sup>,  $R$  is the hydraulic radius, and  $J$  the hydraulic head losses per unit length of pipe, which under the hypothesis of steady-state flow

coincides with that of the pipe bottom line. Known  $v$ , it is possible to calculate the discharge  $Q$  as  $Q=A \cdot v$ , with  $A$  as the transverse section of the pipe.

By setting the Strickler's roughness coefficient to  $90 \text{ m}^{1/3} \cdot \text{s}^{-1}$ , a pipe diameter of 90 mm was obtained for the drains.

As for the collector sizing, by considering the number of single drains flowing to the collector and a total discharge of 4.45 l/s, an average commercial diameter ranging from 250 and 315 mm (DN 250 and DN 315) was selected for each of the BR built in the area.

In summary, in the four farms of the Arborea case study, the drainage network was installed with DN90 pipes using a drain-laying machine (see Figure 4**Error! Reference source not found.**). This can install flexible plastic pipes at depths varying between 50 cm and 200 cm, with automatic control of the lying slope, thus ensuring a gravity flow from drains to the BR. The collectors were installed parallel to the short side of the fields, with a slope toward the lowest point of the ground surface where the BRs have been located.



Figure 4. Some pictures of the operations for drain burying with an automatic drain-lying machine (pictures a and b) in one of the four farms in the Arborea case study, along with connections with the collector (pictures c and d)

#### 4.3. Bioreactors

In general, BRs can be built in-line, utilizing the excavated sections of the existing free-surface channels, or off-line, by creating a properly sized dedicated excavation in areas on the edges of the field and adjacent to the final drainage channel. In the case of in-line bioreactors, the structure is expected to cause a rise in the water level in the upstream drainage channel, potentially leading to backflow from the channel to the drains and, subsequently, to the fields. In the case of the selected farms, the in-line solution was discarded, as the available hydraulic load in the channel would not have been sufficient for normal flow without the occurrence of backflow to the field. Consequently, an off-line solution has been chosen, with the BR positioned at the lower corner of each lot and close to the drainage channel

where the treated water can be discharged. Figure 5 provides a schematic plan view of the drainage network and bioreactor no. 1.



Figure 5. Schematic plan view of the drainage network and bioreactor n. 1. The blue lines indicate the drainage network leading to the BR (in pink in the figure). The BR is located at the lowest point of the field, close to the channel where the treated water is to be discharged.

Since the project aims to define a method that can be extended to the entire Arborea plain, it has been decided to standardize all four bioreactors and build them similarly. The design of the bioreactor has been fundamentally based on two main parameters: the flow rate to be treated and the retention time. While the first is a design value derived from climatic and irrigation management factors, careful evaluation is necessary for the second, as it directly affects the effectiveness of denitrification. Low retention times may not be sufficient to reduce dissolved oxygen to a level that guarantees denitrification, while excessively long times can lead to sulfate reduction and mercury methylation. Based on the above considerations, the BR and its associated works have been sized by considering a retention time falling in a range of 4 to 5 hours and a discharge of 4.5 l/s. Accordingly, each BR has an average width of 4 meters, a length of 25 meters, and a depth of 1.2 meters. Figure 6 provides a schematic view of the BR adopted in the Arborea case study.

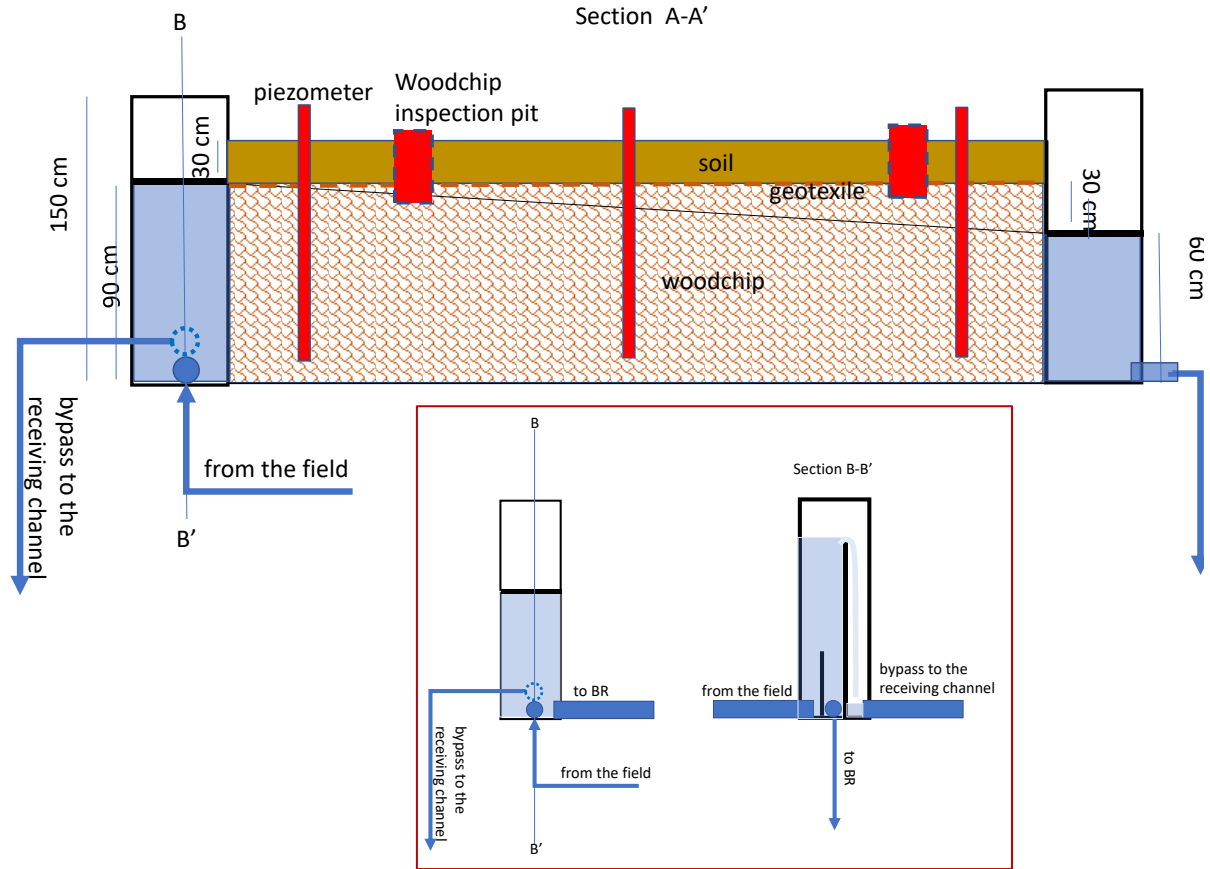


Figure 6. Schematic view of the BR installed in the four farms in the Arborea site, with two sections of the inlet maintenance hole (in the red frame). Drawing not to scale

The walls and the bottom of the excavation have been lined with a 2mm thick HDPE polyethylene waterproof membrane to prevent the percolation of water into the subsoil and covered with a layer of non-woven geotextile (see Figure 7).



Figure 7. some pictures of the pit (pictures a and b) and its lining with the 2mm thick HDPE polyethylene waterproof membrane (picture c). The water in the pit comes from the shallow groundwater and has been pumped out before woodchip filling

Next, the selected carbonaceous substrate (Eucalyptus woodchip) was placed inside the pit created up to a height of 0.90 meters, above which a geotextile layer has been positioned as a separation element from the 30 cm layer of earth covering it (see Figure 8).



Figure 8. A picture of the woodchip filling the BR

The eucalyptus was selected because it is readily available in the area, even if other essences could have also been used, such as Pine or Oak, for example). In general, however, essences with low tannin content

(which would have antiseptic effects) should be preferably used. Other potentially usable materials (such as compost, leaves, starch, cotton, and cellulose) need to be tested, as these materials, typically containing 15-40% lignin, 35-55% cellulose, and 5-25% hemicellulose, could exhibit significantly higher nitrate removal kinetics compared to wood-based materials, as well as provide greater stability and durability of the filtering medium over time.

To ensure a retention time close to the designed one, each BR has been equipped with two manholes: one at the inlet for connection to the drainage collector and one at the outlet to the receiving water body (the channel). Figure 9**Error! Reference source not found.** shows pictures of the inlet and outlet manholes and a 3D drawing of the inlet manhole.

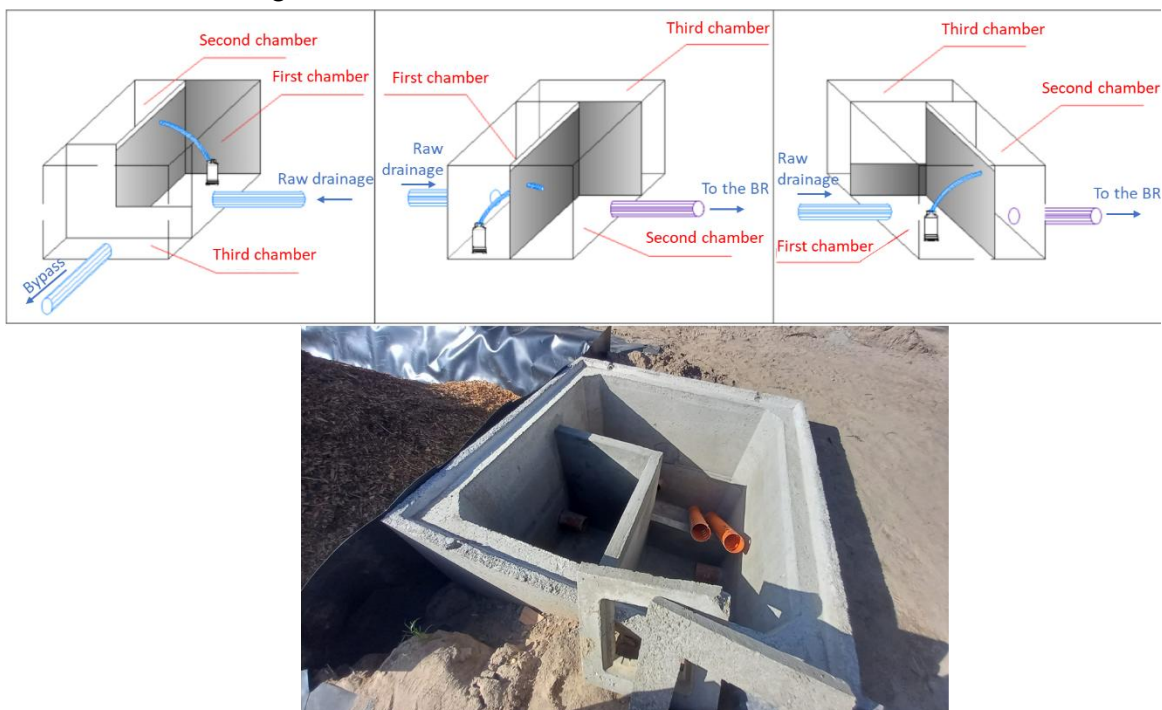


Figure 9. Different perspectives of the inlet three-chamber manhole, along with a photo of an actual inlet structure from one of the bioreactors installed in the Arborea area.

These manholes primarily regulate the hydraulic gradient so that the fluid velocity is not excessive and the retention time remains approximately constant. For this reason, a three-chamber manhole was selected as the upstream manhole: the collector feeds the water into the first chamber, which is equipped with a submersible pump (that pumps the design flow rate to the BR) that lifts the water and directs it into the second chamber, from where the water enters into the BR. The first chamber has a weir that functions as an overflow discharge, directing the water towards the third chamber, from which a connecting pipe leads to the channel to create a bypass line in case the inflow into the manhole exceeds the design flow rate of the bioreactor (which corresponds to the pump's capacity). To minimize

preferential flows into the BR, once in the BR, the water to be treated is evenly distributed across its entire width through a transversal perforated PVC pipe that functions as a diffuser (see Figure 10).



Figure 10. A picture of the transversal perforated PVC pipe diffusing the water to be treated over the whole width of the BR

In the terminal portion of the bioreactor, a perforated PVC similar to that used at the BR inlet has been installed to collect the water over the whole width of the BR and direct it to the outlet manhole. The latter is a two-chamber manhole, with the first chamber receiving the water from the BR and communicating with the second chamber through a weir, whose height may be changed through modular gates, thus allowing the regulation of the hydraulic gradient imposed through the BR. Finally, the treated water is discharged from the second chamber to the final receiving channel. As already mentioned, the modular weir is essential for these systems: on one side, it allows the regulate the velocity (and thus the retention time) at the BR startup when the saturated hydraulic conductivity of the woodchip porous system is not perfectly known; on the other side, it allows adjusting the hydraulic gradient with progressive degradation of the woodchip, which may induce changes in the hydraulic properties of the porous system.

It is worth noting that it is helpful to clarify that both discharges (the bypass of the inlet manhole and the discharge from the outlet manhole) are equipped with an automatic check valve to prevent surface runoff from re-entering the bioreactor. On the other hand, the times for flood formation and those for percolation and reaction differ by at least one order of magnitude, so the interferences should be minimal. All the pictures and videos of different stages of BRs construction in the Arborea site are available at the project website: <https://npp-sol.iamm.ciheam.org/>

## 5. Monitoring

The parameters of interest (Nitrate, Redox Potential, Dissolved Oxygen, Temperature...) are monitored through multiparametric probes installed at the inlet and outlet manholes. Periodic sampling has also been considered for the dual purpose of sensor calibration (the nitrate ion-selective electrode, for example), and additional chemical and microbiological parameters are to be monitored with lower frequencies. Additionally, piezometers installed during the pit filling with woodchip allow for periodic monitoring of the main chemical-microbiological parameters inside the BR through sampling and/or multiparameter probes (see Figure 11).

Finally, a couple of small manholes have also been installed during the filling of the BR to monitor the degradation level of the woodchip in the BR.



Figure 11. A picture showing piezometer installation along the BR

The bioreactor is also equipped with inspection manholes for checking the condition of the wood chips. A bioreactor has an average lifespan of 10-15 years. After this period, the filling material needs to be

replaced. To facilitate the periodic replacement of the carbonaceous substrate, the wood chips can also be laid in the form of gabions, which, at the end of the woodchip operating cycle, can be easily replaced with the help of an excavator."

### 5.1. BR hydraulic performance analysis

One of the key aspects of BRs is achieving the ideal operational hydraulic conditions considered in their design. A way to interpret the complexity of the hydraulic response of an in-situ BR is by carrying out tracer testing. Measuring residence time distribution curves is a straightforward and effective method for assessing the hydraulic performance of an in-situ BR. Tracer analysis helps identify the flow pattern within the BR bed, including potential short-circuiting and preferential flows that could impact residence time. Additionally, it can provide insights into the in-situ effective porosity of the woodchip porous system, which also influences water retention time in the BR.

In tracer studies, a tracer is typically introduced at the BR inlet, and the travel time at the outlet is determined by analyzing effluent samples collected at regular intervals or using automatic analyzers, such as ion-selective electrodes. The tracer injection method affects the shape of the travel time distribution at the outlet. The tracer can be injected as a pulse input, which has to be short enough to be treated mathematically as a Dirac- $\delta$  function, or as a step input, mathematically corresponding to a Heaviside step function, where the tracer is continuously added until the effluent concentration equals the influent concentration. Since the Dirac delta function is the derivative of the Heaviside function, the travel time probability density function from a pulse input can also be obtained by taking the time derivative of the response to a step input.

Various types of tracers can be used to assess the hydraulic performance of BRs. Chloride and bromide are commonly utilized for tracer testing in field-scale beds, column bioreactors with woodchip media, and other systems like wetlands, as they are considered inert chemicals that are not reactive or adsorbed.

The curve of standardized concentrations versus time for a pulse input of tracer (known as Normalised Residence Time Distribution, NRTD, curve) is generally used for analysis. It is obtained by normalizing the measured tracer concentration values, generally by the integral of measured concentrations over time. From the NRTD, some important indices may be drawn that can be used to analyze the hydraulic performance of a BR. In the following section, some of the indices used over the years to characterize output tracer curves will be introduced shortly. Most of these indices have been discussed in detail in Metcalf and Eddy (2014).

### 5.2. Indices used to characterize tracer response curves

#### Mean tracer residence time

The mean tracer residence time,  $t_m$ , is the first normalized moment of the measured NRTD curve (the centroid of the area under the RTD) obtained under steady-state flow:

$$t_m = \frac{\int_0^\infty t C(t) dt}{\int_0^\infty C(t) dt} \approx \frac{\sum t_i C_i \Delta t_i}{\sum C_i \Delta t_i} \quad (20)$$

where  $C_i$  is the outlet tracer concentration measured at time  $t_i$  and  $\Delta t_i$  is the time interval between samplings.

### Variance of tracer residence times

The variance of travel times,  $\sigma_t^2$  is used to define the spread of the RTD and represents the second normalized moment of the distribution

$$\sigma_t^2 = \frac{\int_0^\infty (t - t_m)^2 C(t) dt}{\int_0^\infty C(t) dt} \approx \frac{\sum (t_i - t_m)^2 C_i \Delta t_i}{\sum C_i \Delta t_i} \quad (21)$$

### Tracer mass recovery

The percent tracer recovery is calculated as the ratio of the mass of the tracer recovered at the outlet ( $M_{out}$ ) to the mass of the tracer introduced at the inlet of the BR ( $M_{in}$ )

$$M_{out} = \int_0^\infty Q_{out} C(t) dt \approx \sum Q_{out,i} C_i \Delta t_i \quad (22)$$

where  $Q_{out,i}$  is the discharge measured at the BR outlet at time  $t_i$ . It represents the zeroth moment of the retention time

### Indices related to the theoretical hydraulic retention time

The theoretical hydraulic retention time corresponds to the  $t_t$  obtained by equation 12 (see above). It may be used for calculating interrelated indices of flow uniformity inside the BR, such as short-circuiting index,  $ss_I$ , volumetric efficiency index,  $ve_I$  and skewness of the retention time distribution,  $sk_I$ :

$$ss_I = \frac{t_{in}}{t_t} \quad (23)$$

$$ve_I = \frac{t_m}{t_t}$$

$$sk_I = \frac{t_{50}}{t_t}$$

The index  $ss_I$  is used to measure short-circuiting, with values approaching zero as mixing increases.

A  $ve_I$  value close to 1 suggests that the BR volume is being used effectively, while a value less than 1 indicates uneven flow distribution, for example related due to dead zones. A value greater than 1 signifies physical or chemical retardation (Kadlec and Wallace, 2009).

The  $sk_I$  index is the ratio of the time at which 50% of the tracer is recovered at the BR outlet ( $t_{50}$ ) to the theoretical retention time. A value of 1 indicates a near-Gaussian time distribution, while values greater or smaller than 1 indicate skewness in the retention time distribution.

Times at which 10% and 90% of the tracer has passed through the woodchip bed, respectively and  $t_{90}$ , can be used to calculate the so-called Morril dispersion index,  $MD_I$ , which is a dispersion index similar to the previous ones

$$MD_I = \frac{t_{90}}{t_{10}} \quad (24)$$

The  $ve_I$  obtained by a tracer test may thus be used to correct the theoretical hydraulic retention time calculated under the actual operative conditions of the BR, to yield the actual hydraulic retention time,  $t_a = ve_I t_t$

### In-situ effective porosity and saturated hydraulic conductivity

After calculating  $t_m$  from the tracer test, the in-situ effective porosity of the beds is estimated as

$$\phi_e = \frac{Qt_m}{V_s} = \frac{q_w t_t}{L} \quad (25)$$

Finally, the saturated hydraulic conductivity of the woodchip bed may be calculated by inverting equation 10 either under tracer test or operative conditions.

## 6. Maintenance

The designed BR does not require intensive maintenance. In general, it will be mostly limited to the following operations:

Periodic sediment removal from the sediment chamber of the inlet manhole. The frequency will depend on the size of the basin and the amount of sediment entering the structure, but it will generally be

annually or after flood events. Leaves and grass in the sediment chamber should be removed to maintain capacity.

The outlet structure should be monitored regularly to check for blockages, and any blockages should be cleared. Grass, sediment build-up, and debris should be kept clear of the outlets so water can freely discharge from the BR.

Replacement of woodchips. As mentioned, the BRs are equipped with inspection manholes to check the condition of the woodchips. The woodchips will gradually degrade and need to be topped up or replaced. The timing of replacement will depend on the material and environmental conditions such as temperature, wetting and drying regimes. To facilitate the periodic replacement of the carbonaceous substrate, the wood chips can also be laid in the form of gabions, which, at the end of the woodchip operating cycle, can be easily replaced with the help of an excavator."

## 7. Summary of the parameters used for BR design

### Woodchip characteristics

- Porosity:  $0.6 < \varphi < 0.7$ ;
- Density (bed already in place):  $200 < \rho_b < 270 \text{ kg/m}^3$ ;
- Saturated hydraulic conductivity:  $0.035 < K_s < 1.1 \text{ ms}^{-1}$ ;
- Equivalent average diameter:  $20 \text{ mm} < D_c < 50 \text{ mm}$ ;
- C:N ratio:  $300:1 < \text{C:N} < 3000:1$ ;
- Low tannin content

### Design parameters

Once the drainage system has been designed (drain depth, spacing, etc.), the peak flow rate  $Q_p$  is determined according to the method described in the drainage design, which represents the flow rate expected from the drainage system under peak operating conditions (for a drainage coefficient between 10 and 12 mm/day). The design flow rate  $Q$ , which needs to be treated, is then determined to be approximately 20% of  $Q_p$ . The nominal flow rate  $Q_n$  is the amount that the bioreactor can handle, given the hydraulic gradient imposed between the inlet and outlet of the bioreactor and the saturated conductivity of the porous medium, and must ensure the passage of the design flow rate  $Q$ .

Drainage factor:  $DF=12 \text{ mm/d}$

Peak discharge, calculated by the DF criterium:  $Q_p=1920 \text{ m}^3/\text{d}$

Design Discharge:  $Q=0.2Q_p = 384 \text{ m}^3/\text{d}$

Nominal Discharge:  $Q_n=384 \text{ m}^3/\text{d}=4.45 \text{ l/s}$

Hydraulic load difference:  $\Delta H=0.3 \text{ m}$

BR length:  $L=25 \text{ m}$

BR width:  $W=4\text{m}$

Half-path hydraulic load (in the case of constant piezometric slope:  $0.75 \text{ m}$ )

Hydraulic gradient:  $\Delta H/L= 0.012$

Wetted area at the half-path:  $WA=3 \text{ m}^2$

Average retention time  $\tau$  (hours):  $4 \div 6 \text{ hours}$

Nitrate Removal efficiency:  $NRe=1 \text{ g N/m}^3/\text{d}$  (increased by integrating the woodchip with methanol, acetates, ...)

## 8. References

Borno M.L., Muller-stover D.S., Liu F. 2018. Contrasting effects of biochar on phosphorus dynamics and bioavailability in different soil types. *Sci. Total Environ.*, 627, pp. 963-974.  
<https://doi.org/10.1016/j.scitotenv.2018.01.283>

Camilo, B.K., A. Matzinger, N. Litz, L.P. Tedesco, G. Wessolek, 2013. Concurrent nitrate and atrazine retention in bioreactors of straw and bark mulch at short hydraulic residence times, *Ecological Engineering*, Volume 55, 2013, Pages 101-113, ISSN 0925-8574,  
<https://doi.org/10.1016/j.ecoleng.2013.02.010>.

Christianson, L. E., Wickramarathne, N., Johnson, G. M., & Feyereisen, G. W. (2022). No/low-cost chipped woody debris nutrient composition benefits and tradeoffs for denitrifying bioreactors. *Bioresource Technology Reports*, 20, 101237. <https://doi.org/10.1016/j.biteb.2022.101237>

Christianson, L., J. Tyndall, M. Helmers, 2013. Financial comparison of seven nitrate reduction strategies for Midwestern agricultural drainage - *Water Resources and Economics*, 2013

Christianson, L.E., Castello, A., Christianson, R., Helmers, M., Bhandari, A. 2010. Hydraulic property determination of denitrifying bioreactor fill media. *Applied Engineering in Agriculture* 26(5):849-854

Christianson, L.E., Lepine, C., Sibrell, P.L., Penn, C., Summerfelt, S.T. 2017. Denitrifying woodchip bioreactor and phosphorus filter pairing to minimize pollution swapping. *Water Research* 121:129-139.

Coleman B. S.L., Z.M. Easton and E. M. Bock, 2019. Biochar fails to enhance nutrient removal in woodchip bioreactor columns following saturation. *Journal of Environmental Management* Volume 232, Pages 490-498

Coleman, B.S.L., Easton, Z. M., Bock, E.M. 2019. Biochar fails to enhance nutrient removal in woodchip bioreactor columns following saturation. *Journal of Environmental Management* 232:490-498.

Ghane, E., Fausey, N.R., Brown, L.C., 2014. Non-Darcy flow of water through woodchip media. *J. Hydrol.* 519, 3400–3409.

Ghane, E., Fausey, N.R., Brown, L.C., 2015. Modeling nitrate removal in a denitrification bed. *Water Res.* 71, 294–305.

Goodwin G.E., Bhattarai R., Cooke R. 2015. Synergism in nitrate and orthophosphate removal in subsurface bioreactors. *Ecol. Eng.*, 84 (2015), pp. 559-568, [10.1016/j.ecoleng.2015.09.051](https://doi.org/10.1016/j.ecoleng.2015.09.051)

Gottschall, N., Edwards, M., Craiovan, E., Frey, S. K., Sunohara, M., Ball, B., Zoski, E., Topp, E., Khan, I., Clark, I. D., & Lapen, D.R. (2016). Amending woodchip bioreactors with water treatment plant residuals to treat nitrogen, phosphorus, and veterinary antibiotic compounds in tile drainage. *Ecological Engineering*, 95, 852–864. <https://doi.org/10.1016/j.ecoleng.2016.06.011>

Greenan, C.M., Moorman, T.B., Kaspar, T.C., Parkin, T.B., Jaynes, D.B. 2006. Comparing carbon substrates for denitrification of subsurface drainage water. *Journal of Environmental Quality* 35(3):824-829.

Griesmeier, V., Bremges, A., McHardy, A. C., & Gescher, J. (2017). Investigation of different nitrogen reduction routes and their key microbial players in wood chip-driven denitrification beds. *Scientific Reports*, 7(1), 17028. <https://doi.org/10.1038/s41598-017-17312-2>

Halaburka, B.J., LeFevre, G.H., Luthy, R.G., 2017. Evaluation of mechanistic models for nitrate removal in woodchip bioreactors. *Environ. Sci. Tech.* 51 (9), 5156–5164.

Hassanpour B., L. D. Geohring, A. R. Klein, S. Giri, L. Aristilde, T. S. Steenhuis, 2019. Application of denitrifying bioreactors for the removal of atrazine in agricultural drainage water. *Journal of Environmental Management*, Volume 239, 2019, Pages 48-56, ISSN 0301-4797, <https://doi.org/10.1016/j.jenvman.2019.03.029.>)

Hooghoudt, S.B. 1940. General consideration of the problem of field drainage by parallel drains, ditches, watercourses, and channels. Publ. No.7 in the series Contribution to the knowledge of some physical parameters of the soil (titles translated from Dutch). Bodemkundig Instituut, Groningen, The Netherlands)

Hua G., Salo M.W., Schmidt C.G., Hay C.H. 2016. Nitrate and phosphate removal from agricultural subsurface drainage using laboratory woodchip bioreactors and recycled steel byproduct filters. *Water Res.*, 102 (2016), pp. 180-189, [10.1016/j.watres.2016.022](https://doi.org/10.1016/j.watres.2016.022)

Hunter W. J., D.L. Shaner, 2010. Biological remediation of groundwater containing both nitrate and atrazine. *Curr. Microbiol.*, 60 (2010), pp. 42-46, [10.1007/s00284-009-9499-3](https://doi.org/10.1007/s00284-009-9499-3)

Husk, B. R., J.S. Sanchez, B.C. Anderson, J.K. Whalen and B.C. Wootton *Journal of Soil and Water Conservation*. 2018, 73 (3) 265-275; DOI: <https://doi.org/10.2489/jswc.73.3.265>).

IDALS, IDNR, ISUCALS, 2017. Iowa Department of Agriculture and Land Stewardship, Iowa Department of Natural Resources, Iowa State University College of Agriculture and Life Sciences, 2017. Iowa nutrient reduction strategy)  
[https://publications.iowa.gov/39714/1/2017%20INRS%20Complete\\_Revised%202017\\_12\\_11.pdf](https://publications.iowa.gov/39714/1/2017%20INRS%20Complete_Revised%202017_12_11.pdf)

Ilhan, Z.E., Ong, S.K., Moorman, T.B., 2011. Dissipation of atrazine, enrofloxacin, and sulfamethazine in wood chip bioreactors and impact on denitrification. *J. Environ. Qual.* 40, 1816. <https://doi.org/10.2134/jeq2011.0082>.

Laird D., Fleming P., Wang B., Horton R., Karlen D., 2010. Biochar impact on nutrient leaching from a Midwestern agricultural soil, *Geoderma*, Volume 158, Issues 3–4, 2010, Pages 436-442, ISSN 0016-7061, <https://doi.org/10.1016/j.geoderma.2010.05.012>.

Martin, E. A., Davis, M. P., Moorman, T. B., Isenhart, T. M., & Soupir, M. L. (2019). Impact of hydraulic residence time on nitrate removal in pilot-scale woodchip bioreactors. *Journal of Environmental Management*, 237(3), 424–432. <https://doi.org/10.1016/j.jenvman.2019.05.022>

Metcalf and Eddy, 2014 *Wastewater Engineering: Treatment and Resource Recovery*. McGraw-Hill, New York, NY, USA).

Perera, G. N., Rojas, D. T., Rivas, A., Barkle, G., Moorhead, B., Schipper, L. A., Craggs, R., & Hartland, A. (2024). Elucidating phosphorus removal dynamics in a denitrifying woodchip bioreactor. *Science of the Total Environment*, 917, 170478. <https://doi.org/10.1016/j.scitotenv.2024.170478>

Rambags, F., Tanner, C., & Schipper, L. (2019). Denitrification and anammox remove nitrogen in denitrifying bioreactors. *Ecological Engineering*, 138, 38–45.

<https://doi.org/10.1016/j.ecoleng.2019.06.022>

Rich, J.J., Heichen, R.S., Bottomley, P.J., Cromack Jr., K., Myrold, D.D. 2003. Community composition and functioning of denitrifying bacteria from adjacent meadow and forest soils. *Applied and Environmental Microbiology* 69(10):5974-5982.

Rivas, A., Barkle, G., Stenger, R., Moorhead, B., Clague, J., 2020. Nitrate removal and secondary effects of a woodchip bioreactor for the treatment of subsurface drainage with dynamic flows under pastoral agriculture. *Ecol. Eng.* 148, 105786. <https://doi.org/10.1016/j.ecoleng.2020.105786>.

Robertson, W.D., Merkley, L.C. 2009. In-stream bioreactor for agricultural nitrate treatment. *Journal of Environmental Quality* 38:230-237.

Sanchez Bustamante-Bailon, A. P., Margenot, A., Cooke, R. A. C., & Christianson, L. E. (2022). Phosphorus removal in denitrifying woodchip bioreactors varies by wood type and water chemistry. *Environmental Science and Pollution Research*, 29(5), 6733–6743. <https://doi.org/10.1007/s11356-021-15835-w>

Sanchez Bustamante-Bailon, A. P., Margenot, A., Cooke, R. A. C., & Christianson, L. E., 2022. Phosphorus removal in denitrifying woodchip bioreactors varies by wood type and water chemistry. *Environmental Science and Pollution Research*, 29(5), 6733–6743. <https://doi.org/10.1007/s11356-021-15835-w>

Sarris, T.S., Burberry, L.F., 2018. Stochastic multi-objective performance optimization of an instream woodchip denitrifying bioreactor. *Ecological Engineering* 124:38-50.

Schipper, L.A., Robertson, W.D., Gold, A.J., Jaynes, D.B., Cameron, S.C. 2010. Denitrifying bioreactors – an approach for reducing nitrate loads to receiving waters. *Ecological Engineering* 36:11(1532-1543).

von Ahnen, M., Pederson, P.B., Dalsgaard, J., 2016. Start-up performance of a woodchip bioreactor operated end-of-pipe at a commercial fish farm—a case study. *Aquac. Eng.* 74, 96–104. <https://doi.org/10.1016/j.aquaeng.2016.07.002>

White, S. A., Morris, S. A., Wadnerkar, P. D., Woodrow, R. L., Tucker, J. P., Holloway, C. J., Conrad, S. R., Sanders, C. J., Hessey, S., and Santos, I. R. (2022). Anthropogenic nitrate attenuation versus nitrous oxide release from a woodchip bioreactor. *Environmental Pollution*, 300, 118814.

<https://doi.org/10.1016/j.envpol.2022.118814>

Zoski E.D., Lapen D.R., Gottschall N., Murrell R.S., Schuba B. 2013. Nitrogen, phosphorus, and bacteria removal in laboratory-scale woodchip bioreactors amended with drinking water treatment residuals *Trans. ASABE*, 56 (4) (2013), pp. 1339-1347, 10.13031/trans.56.9836